HHS Public Access

Author manuscript

Neurobiol Aging. Author manuscript; available in PMC 2016 March 01.

Published in final edited form as:

Neurobiol Aging. 2015 March ; 36(3): 1569–1576. doi:10.1016/j.neurobiolaging.2014.11.017.

Effects of aging on glutamate neurotransmission in the substantia nigra of *Gdnf* heterozygous mice

Ariana Q Farrand[1,*], **Rebecca A Gregory**[2,*], **Michael D Scofield**[1], **Kristi L Helke**[2], and **Heather A Boger**[1]

[1]Department of Neurosciences, Medical University of South Carolina, Charleston, SC, 29425

[2]Department of Comparative Medicine, Medical University of South Carolina, Charleston, SC, 29425

Abstract

Glial cell line-derived neurotrophic factor (GDNF) helps protect dopaminergic neurons in the nigrostriatal tract. Although the cause of nigrostriatal degeneration is unknown, one theory is that excess glutamate from the subthalamic nucleus (STN) results in excitotoxic events in the substantia nigra (SN). Since dopaminergic degeneration is accompanied by a reduction in GDNF, we examined glutamate neurotransmission in the SN using a *Gdnf* heterozygous mouse model (*Gdnf*$^{+/-}$) at 8 and 12 months of age. At 8 months, *Gdnf*$^{+/-}$ mice have greater glutamate release and *higher basal glutamate levels*, which precede the SN dopaminergic degeneration observed at 12 months of age. However, at 12 months, *Gdnf*$^{+/-}$ mice have lower basal levels of glutamate and less glutamate release than wildtype (WT) mice. Also at 8 months, *Gdnf*$^{+/-}$ mice have lower levels of GLT-1 and greater GFAP levels in the SN compared to WT mice, differences that increase with age. These data suggest that reduced levels of GDNF induce excess glutamate release and dysregulation of GLT-1, causing excitotoxicity in the SN that precedes dopaminergic degeneration.

Keywords

In vivo electrochemistry; glutamate; glial cell-line derived neurotrophic factor (GDNF); substantia nigra; striatum; neurodegeneration

1. Introduction

Glial cell line-derived neurotrophic factor (GDNF) is an important growth factor for the development, survival, and maintenance of midbrain dopaminergic (DAergic) neurons (Lin

Corresponding author: Heather A. Boger, PhD, Medical University of South Carolina, 173 Ashley Avenue, BSB Suite 403, MSC 510, Charleston, SC 29425 USA, boger@musc.edu.

*Authors contributed equally to experiments and manuscript

et al., 1993, Deister and Schmidt, 2006). The nigrostriatal DAergic system is involved with motor function, both of which decline with normal aging (Volkow et al., 1998; Ingram, 2000). Individuals with Parkinson's disease (PD) experience an accelerated decline in the DAergic system resulting in greater motor impairment (Jenner and Olanow, 1998, Jankovic, 2008). While GDNF levels are reduced in the surviving dopamine (DA) neurons of PD patients (Chauhan et al., 2001), GDNF administration has been shown to exert neuroprotective and neurorestorative effects on substantia nigra (SN) DA neurons in animal models of PD (Borlongan et al., 2001; McGrath et al., 2002), as well as in PD patients (Gill et al., 2003; Slevin et al., 2005).

A mouse model with a partial knockout of the *Gdnf* gene was produced to study the impact GDNF has on DAergic systems (*Gdnf*$^{+/-}$; Pichel et al., 1996). *Gdnf*$^{+/-}$ mice have a 40% reduction in GDNF protein levels (Boger et al., 2006). Previous studies from our laboratory have demonstrated that *Gdnf*$^{+/-}$ mice have an accelerated decline in motor function and DAergic dysfunction compared to wildtype (WT) mice (Boger et al., 2006). *Gdnf*$^{+/-}$ mice also have greater levels of nigral inflammation and oxidative stress, both of which have been implicated in DAergic neurodegeneration (Boger et al., 2007; Littrell et al., 2013). Acute intra-striatal administration of GDNF attenuated these effects, prevented DAergic cell loss, and improved motor function (Littrell et al., 2013). Taken together, these data continue to demonstrate the importance of GDNF to DA systems. However, the mechanism by which GDNF exerts its neuroprotective effects is still unknown.

A potential mechanism for the accelerated decline of nigrostriatal DA in *Gdnf*$^{+/-}$ mice is glutamate neurotransmission dysfunction. Glutamatergic neurons of the subthalamic nucleus (STN) project to the SN (Iribe et al., 1999). Previous studies have shown that glutamate can become toxic if it remains in the synaptic cleft (Mark et al., 2004; Sonsalla et al., 1992). This excitotoxicity, which may be caused by either excess presynaptic release or decreased glutamate uptake by transporters, leads to continuous post-synaptic glutamate receptor activation. Overactive receptors will increase the release of intracellular calcium, leading to oxidative stress (Joseph et al., 2002; Kruman and Mattson, 1999) followed by inflammatory events (Blandini et al., 1996; Gianforcaro and Hamadeh, 2014). The excess calcium depletes energy stores *and may* result in DA cell death (Gordon, 2013; Misonou et al., 2006).

Several studies have been conducted to explore a link between GDNF and glutamate. Activation of glutamate receptors in various animal models of neurological disorders has been shown to increase GDNF levels in the brain (Di Liberto et al., 2011; Kosuge et al., 2009). Another study suggests that increased levels of GDNF may help protect neurons from excitotoxic death (Ho et al., 1995). Based on these previous findings, we focused our studies on the potential impact that a GDNF reduction has on glutamate neurotransmission and inflammation with age. We hypothesized that mice with a partial reduction of GDNF have increased glutamate neurotransmission in the SN that precedes the motoric and DAergic loss observed *in previous studies* at 12 months of age (Boger et al., 2006, Littrell et al., 2013). Therefore, in this study we assessed KCl-stimulated glutamate release and uptake in the SN of 8- and 12-month old *Gdnf*$^{+/-}$ and WT mice. Additionally, we assessed various markers of the glutamatergic system, including glutamate transporter-1 (GLT-1), vesicular glutamate transporter 2 (VGLUT-2), and glial fibrillary acidic protein (GFAP).

2. Materials and Methods

2.1. Animals

For these experiments, heterozygous 8- and 12-month-old (mon) male B6.Cg-*Gdnf*^{tm1Lmgd} (*Gdnf*$^{+/-}$) mice were compared with their WT littermates (N=5–8/genotype/group) (Pichel et al., 1996). *Gdnf*$^{+/-}$ offspring containing this allele are fertile and viable, whereas *Gdnf* homozygous knockouts are embryonic lethal. This mouse colony was established at the Medical University of South Carolina (MUSC) according to National Institutes of Health (NIH)-approved protocols. Mice for this study were bred at MUSC and backcrossed for greater than 10 generations onto a C57BL/6J background. Mice were weaned and genotyped as previously described (Boger et al., 2006). The mice were housed three to five animals per cage with a twelve hour light/dark cycle. The room was kept at 20–22°C, and food and water were provided ad libitum.

2.2. Enzyme-Based Glutamate Biosensor

S2 ceramic-based microelectrode arrays (MEA) were prepared for in vivo recordings (Burmeister et al., 2002; Quintero et al., 2011). Briefly, recording sites were coated with a glutamate oxidase (GluOx) enzyme solution (U.S. Biological) containing a final concentration of 1% bovine serum albumin (BSA, Sigma-Aldrich), 0.125% glutaraldehyde (Sigma-Aldrich), and 1% GluOx. After a 24-hour (hr) drying period, platinum sites were electroplated with an m-Phenylenediamine dihydrochloride size exclusion layer (Acros Organics) to block potential interfering analytes such as ascorbic acid (AA), catecholamines and indoleamines (Burmeister et al., 2002; Hascup et al., 2008). The GluOx enzyme is required for measurement of glutamate as it metabolizes glutamate to α-ketoglutarate, which is then converted to the reporter molecule hydrogen peroxide (H_2O_2). When a potential of +0.7 V versus a silver/silver chloride reference electrode was applied to the MEA, H_2O_2 is oxidized resulting in the transfer of two electrons to the platinum recording surface. The resulting change in current was amplified and digitized by a FAST16 MKIII recording system (Quanteon, LLC).

2.3. Electrode Calibration

MEAs were calibrated to determine their sensitivity to glutamate and selectivity against AA using constant potential amperometry with a FAST16 MKIII system as described previously (Burmeister et al., 2002; Quintero et al., 2011). Briefly, the MEA was submerged in 40 mL of a continuously stirred solution of 0.05 M phosphate-buffered saline filtered and titrated to pH 7.4 and allowed to reach a stable baseline for ~60 minutes (min) before calibrating. Phosphate buffer temperature was maintained at 37°C using a circulating water bath (Gaymar Industries). Aliquots of freshly made 20 mM AA and 20 mM glutamate were used to obtain final concentrations of 250 μM AA and 20, 40, and 60 μM glutamate for all calibrations. Selectivity ratios for glutamate over AA were calculated in addition to the limit of detection (LOD) and linearity (R^2) for all glutamate MEAs. Reported as mean ±S.E.M., the MEAs had average selectivity ratios of 35 ± 13: 1, limits of detection (LOD) of 0.8 ± 0.4 μM and R^2 values of 0.9983 ± 0.002. The MEAs were also tested to compare the recording capability among the platinum recording sites using H_2O_2 (8.8 μM, final concentration) as a test substance. Electrodes that did not respond to H_2O_2, had R^2 values <0.99, or had LODs

>5 μM were excluded. After calibration, MEAs were fitted with single-barrel glass capillaries that were pulled and bumped to an inner tip diameter of approximately 10 μm. The pipette was attached under a dissection scope in order to place the tip of the pipette above the glutamate sensitive sites, 75 μm from the surface of the MEA (Burmeister et al., 2002; Smith et al., 2007). The pipette was filled with freshly made KCl solution containing 70 mM KCl, 79 mM NaCl, and 2.5 mM $CaCl_2$ at pH 7.4, attached to the headstage, and connected to a Picospritzer III (Parker Instruments).

2.4. In Vivo Glutamate Electrochemistry

The electrode was implanted into the mouse SN (Hoffman and Gerhardt, 1998). Mice were anesthetized with 12.5% urethane at 0.01 mL/g body weight injection volume and placed in a stereotaxic apparatus (David Kopf Instruments) fitted with a 37°C heating pad. Following removal of the scalp tissue, mice underwent a craniotomy, leaving bregma intact. Mice were implanted with a glutamate-selective MEA-KCl pipette assembly into the left and right SN (AP, −3.0 mm; ML, ±1.25 mm; DV, −4.2 mm relative to bregma; Franklin and Paxinos, 2001; Fig. 1*A*). A small hole was drilled at the front of the skull above the parietal cortex for placement of the silver/silver chloride reference electrode. Once the MEA was lowered, mice underwent a minimum of 30 min acclimation period to establish a stable baseline recording. Following baseline period, pressure ejections of 70 mM KCl solution were performed using the Picospritzer III microinjection dispensing system. Approximately 150 nL of KCl solution was pressure ejected adjacent to the microelectrode to induce depolarization and subsequent release of glutamate into the SN. KCl ejection resulted in reproducible glutamate peaks detected by MEAs. Following each KCl ejection, recordings were allowed to return to baseline for at least 3 min before repeating the procedure. This procedure was repeated 6–8 times for each recording site. *Following recordings, the brains were processed for immunohistochemical detection and electrode placement in the SN was verified via microscope on sections stained for TH for each animal (*Fig. 1B).

2.5. Electrochemistry Data Analysis

The FAST16 MKIII recording system saved amperometric data, time, and experimenter mediated ejection marks. All data traces from MEAs were analyzed with the FAST Analysis software (Jason Burmeister Consulting, LLC), a program written and compiled in Matlab from Mathworks. The FAST Analysis software was used to determine basal glutamate (μM), peak amplitude (glutamate release, μM), and k_{-1} (glutamate uptake, sec^{-1}), *see* Fig. 1C for representative traces. All data were passed through a low stringency wavelet low pass filter (using the Daubechies wavelet) to remove high frequency noise.

2.6. Brain Preparation

Upon completion of electrochemical recordings, the mice were decapitated while deeply anesthetized. The brains were extracted and dissected. Samples from the right dorsal striatum were dissected and stored at −80°C for Western blotting. The left and right caudal portion of the brain containing both STN and SN was blocked and placed in 4% paraformaldehyde at 4°C. After 48 hr, the STN/SN tissue block was placed in 30% sucrose for at least 24 hr before cryo-sectioning for immunohistochemistry (45 μm; Microm).

2.7. Immunohistochemical Staining

Immunohistochemistry in the SN was performed using rabbit polyclonal glial fibrillary acidic protein antibody (GFAP; 1:2000 Dako) or rabbit polyclonal GLT-1 (1:1000 Abcam). Immunohistochemistry in the STN was performed using a guinea pig polyclonal VGLUT-2 (vesicular glutamate transporter-2) antibody (1:20,000 Millipore). Briefly, primary antibodies were applied to serial sections taken every 6th section from the SN or STN based on our previous protocols (Boger et al., 2006). Endogenous peroxidase activity was quenched by treating sections with 10% H_2O_2 in 20% methanol for 10 min. Sections were then permeabilized in TBST (TBS with 0.25% TritonX-100) following treatment for 20 min with sodium meta-periodate. Non-specific binding was controlled by incubation in 10% normal goat serum (NGS) for 1 hr. Sections were then incubated overnight in the primary antibody at room temperature. The next day, sections were incubated for 1 hr with the secondary antibody (1:200; biotinylated goat anti-rabbit serum or biotinylated goat anti-guinea pig serum, Vector Laboratories) and 1 hr with avidin-biotin complex (ABC kit, Vector labs). The reaction was developed using VIP peroxidase substrate kit (Vector labs) to enhance the reaction and produce a color stain. This reaction was stopped using 0.1 M phosphate buffer, and the sections were mounted on glass slides, dehydrated and cover-slipped with DPX (Sigma). *To control for staining intensity, staining of all sections for each antibody were conducted on the same day, and developed with VIP for the same amount of time (GFAP: 3 min, GLT-1: 0.5 min, VGLUT-2: 1 min).*

2.8. Semiquantitation of GLT-1, GFAP, and VGLUT-2 immunostaining

Staining intensity of VGLUT-2 in the STN, and GLT-1 and GFAP in the SN, was determined using NIH Image J Software to measure a gray scale value within the range of 0–256, where 0 represents white and 256 black. A template for the SN and STN was created and used on all brains similarly, and images were captured with a Nikon Eclipse E-600 microscope, or an Olympus-750 video camera system, and a Dell Pentium III computer. Measurements were performed blinded and measurements from 4 sections per brain region (STN or SN) were averaged to obtain one value per subject. Staining density was obtained when background staining was subtracted from mean staining intensities on every 6th section through the STN (VGLUT-2) and SN (GLT-1 and GFAP).

2.9. Immunoblotting

Samples of right dorsal striatum were homogenized on ice using lysis buffer containing PhosSTOP (Roche) and Protease Inhibitor (CalBiochem), and then loaded in duplicate (15 μg) and separated on Mini-PROTEAN TGX gels (BioRad Laboratories) at 200 V for 35 min. Proteins were transferred onto a polyvinylidene difluoride (PVDF) membrane (BioRad Laboratories) via a semi dry transfer for 7 min using 2.5 A and 25 V. The membranes were removed from the cassette and blocked in 5% non-fat milk for 1 hr at room temperature. The blots were then incubated overnight at 4°C in the primary antibodies (GLT-1 1:5000, Abcam; GFAP 1:30,000, Abcam; TH 1:500, PelFreez). The next day, the blots were rinsed in PBS with 0.1% Tween-20 (PBSt) and incubated in the secondary antibody (peroxidase-conjugated goat anti-rabbit IgG 1:10,000) for 1 hr. After repeating the PBSt rinse, blots were imaged on a Kodak Image Station (3 exposures) using SuperSignal West Dura Luminol/

Enhancer Solution (Thermo Scientific Laboratories). The band intensities were normalized for protein load in each well. Normalized intensities of each band were reported as percent of the WT whole-brain control sample that was run on each blot.

2.10. Statistical Analysis

Electrochemical, western blot, and immunohistochemical data were analyzed utilizing a 2 (genotype) × 2 (age) mixed-factor ANOVA analysis using Statview. For multiple comparisons of groups, data were analyzed using one-way ANOVA comparisons, followed by Fisher's PLSD post-hoc analysis. Significance is reported as $p<0.05$.

3. Results

3.1. Alterations in glutamate kinetics in *Gdnf*$^{+/-}$ mice

The glutamate system of the basal ganglia has been closely linked to neurodegenerative diseases. In this study, we examined glutamate neurotransmission in the SN using in vivo electrochemical detection to determine if glutamate neurotransmission was altered. A 2 (genotype) × 2 (age) ANOVA showed a significant interaction between genotype and age on basal glutamate levels ($F_{(1,22)}=9.481$; $p<0.01$). A group-wise comparison indicated a significant difference ($F_{(3,22)}=4.410$; $p<0.05$). A Fisher's post-hoc analysis showed that 8 mon *Gdnf*$^{+/-}$ mice have higher basal glutamate than WT mice at 8 mon ($p<0.05$) and *Gdnf*$^{+/-}$ mice at 12 mon ($p<0.01$), and lower glutamate baseline levels in 12 mon *Gdnf*$^{+/-}$ mice than WT mice at 12 mon ($p<0.05$; Fig. 1*B*). These data indicate that at 8 mon, *Gdnf*$^{+/-}$ mice have higher levels of glutamate in the extracellular space than age-matched WT mice. However, at 12 mon, there is less glutamate in the extracellular space of *Gdnf*$^{+/-}$ mice as opposed to WT mice ($p<0.05$).

In addition, we looked at the magnitude of glutamate release as a potential cause of glutamate excitotoxicity in *Gdnf*$^{+/-}$ mice compared to WT mice. Glutamate release was measured by the maximum peak amplitude of the evoked response to 70 mM KCl (Morris et al., 2011) applied locally in the SN. A 2 (genotype) × 2 (age) ANOVA showed that KCl-stimulated glutamate release is affected by age ($F_{(1,18)}=4.832$; $p<0.05$), and a genotype x age interaction existed ($F_{(1,18)}=8.912$; $p<0.01$). A group-wise comparison indicated a significant difference between groups ($F_{(3,18)}=5.144$; $p<0.01$). Eight mon *Gdnf*$^{+/-}$ mice released significantly more glutamate than 12 mon *Gdnf*$^{+/-}$ mice ($p<0.01$) and more than 8 mon WT mice ($p<0.05$; Fig. 1*C*). At 12 mon, *Gdnf*$^{+/-}$ mice had less glutamate release compared to WT mice, although not statistically significant ($p=0.0573$).

Glutamate excitotoxicity can occur when excess glutamate persists in the synaptic cleft, and in the extracellular space. This excess glutamate causes receptors on the post-synaptic neuron to remain over-activated, and can also eventually lead cell death (Manev et al., 1989; Misonou et al., 2006). *In this study we examined glutamate uptake by measuring* k_{-1} *(with units of* sec^{-1}*), the decay constant for glutamate clearance* (Burmeister and Gerhardt, 2001). A 2 (genotype) × 2 (age) ANOVA showed that the *Gdnf*$^{+/-}$ genotype had a significant effect on glutamate clearance ($F_{(1,19)}=8.519$; $p<0.01$); however, neither age nor interaction between the two main effects existed. A group-wise comparison confirmed that there was a significant difference between the groups ($F_{(3,19)}=3.459$; $p<0.05$). A Fisher's post-hoc

analysis showed that there was no significant difference between genotypes at 8 mon, even though there is a trend towards *Gdnf*$^{+/-}$ mice having slower clearance, but at 12 mon, *Gdnf*$^{+/-}$ mice had significantly slower glutamate clearance (uptake) than age-matched WT mice ($p<0.05$; Fig. 1*D*). Taken together, the *increased basal levels and release* suggest that *Gdnf*$^{+/-}$ mice have alterations in glutamate transmission at an age prior to SN DA loss (Boger et al., 2006; Littrell et al., 2013), suggesting a role for excess glutamate in the degeneration of this system.

3.2. Effects of aging and reduced GDNF on GLT-1 and GFAP in the SN

GLT-1, a glutamate transporter primarily expressed on astrocytes, is responsible for removing glutamate from the synaptic cleft as well as from the extrasynaptic space. We wanted to assess levels of this transporter in the SN to evaluate its role as a potential mechanism for DAergic cell death due to glutamate excitotoxicity in *Gdnf*$^{+/-}$ mice. A 2 (genotype) × 2 (age) ANOVA found overall genotype ($F_{(1,16)}=21.47$; $p<0.001$) and age effects ($F_{(1,16)}=40.433$; $p<0.0001$), but interaction of the two factors did not exist. A group-wise comparison showed a significant difference between the groups ($F_{(3,16)}=21.2$; $p<0.0001$). A Fisher's PLSD post hoc analysis found that GLT-1-immunoreactivity (ir) decreased in both genotypes with age (WT: $p<0.01$; *Gdnf*$^{+/-}$: $p<0.0001$), and *Gdnf*$^{+/-}$ mice had less GLT-1-ir than WT mice at both ages (8 mon: $p<0.05$; 12 mon: $p<0.0.001$; Fig. 2*A*–*E*). These data coupled with reduced glutamate uptake *at 12 mon* suggests that dysfunction of glutamate clearance mechanisms of *Gdnf*$^{+/-}$ mice potentially results in DAergic cell death as documented in our previous studies (Boger et al., 2006; 2007).

Increased astrogliosis is common with age (Lim et al., 2000); therefore, in this study we assessed GFAP expression in 8 and 12 mon *Gdnf*$^{+/-}$ and WT mice. A 2 (genotype) × 2 (age) ANOVA showed overall age ($F_{(1,26)}=11.687$; $p<0.01$) and genotype effects ($F_{(1,26)}=4.483$; $p<0.05$), but not an interaction of the main factors. A group-wise comparison indicated a significant difference between groups ($F_{(3,26)}=5.627$; $p<0.01$). A Fisher's PLSD post hoc analysis revealed that GFAP-ir density increased in the SN of both genotypes with age (WT: $p<0.05$; *Gdnf*$^{+/-}$: $p<0.05$). At 8 mon, *Gdnf*$^{+/-}$ mice have more GFAP-ir than WT mice ($p<0.05$), but at 12 mon, there is no significant difference between genotypes (Fig. 3*A*–*E*). While some astrogliosis is expected and seen by the increase of GFAP in both genotypes with age, the increase of GFAP-ir in 8 mon *Gdnf*$^{+/-}$ mice compared to 8 mon WT mice indicates that astrogliosis occurs at an earlier age in *Gdnf*$^{+/-}$ mice compared to WT mice.

3.3. Effects of age and GDNF reduction on glutamatergic neurons in the STN

To assess glutamatergic neurons in the STN, we immunolabeled for VGLUT-2, one of the vesicular transporters involved in glutamate neurotransmission, and a marker for glutamatergic neurons (Favier et al., 2013; Varoqui et al., 2002). A 2 (genotype) × 2 (age) ANOVA revealed a significant effect of age on VGLUT-2-ir ($F_{(1,18)}=28.422$; $p<0.0001$), as well as a genotype by age interaction ($F_{(1,18)}=11.962$; $p<0.01$). A group-wise comparison demonstrated a significant difference between groups ($F_{(3,18)}=15.150$; $p<0.0001$). A Fisher's post-hoc analysis showed that there is no significant difference between genotypes at 8 mon. At 12 mon, *Gdnf*$^{+/-}$ mice had significantly lower VGLUT-2-ir than 8 mon *Gdnf*$^{+/-}$ mice ($p<0.0001$) and 12 mon WT mice ($p<0.01$; Fig. 4*A*–*E*). This suggests that the increase in

glutamate release and basal levels are not due to an increase in the number of glutamatergic neurons in the STN, rather a hyperactive glutamate system. The overall decrease in glutamate neurotransmission in 12 mon *Gdnf*$^{+/-}$ mice may be explained by the fact that these mice have fewer glutamatergic neurons in the STN at this age.

3.4. Effects of age and reduced GDNF on TH, GLT-1, and GFAP in the striatum

Since the SN DA neurons project to the striatum, we wanted to assess what effects altered glutamate neurotransmission have on the SN-DA system; therefore, we measured TH levels in the striatum (Fig. 5*A*). A 2 (genotype) × 2 (age) ANOVA found an overall genotype effect ($F_{(1,17)}$=5.998; p<0.05), but not an age effect or an interaction of the two. A group-wise comparison confirmed the difference between groups ($F_{(3,17)}$=3.87; p<0.05). A Fisher's PLSD post hoc analysis revealed that 12 mon *Gdnf*$^{+/-}$ mice had lower levels of TH than both age-matched WT mice (p<0.01) and 8 mon *Gdnf*$^{+/-}$ mice (p<0.05; Fig. 5*A*). The decrease of striatal TH levels in *Gdnf*$^{+/-}$ mice at 12 mon suggests degeneration of the DAergic axons and terminals that project to the striatum from the SN. This result is in accordance with our previous findings of DAergic degeneration in the SN (Boger et al., 2006; Littrell et al., 2013).

The dorsal striatum not only receives signals from the DAergic neurons of the SN, but also from cortical glutamate neurons (Fieblinger et al., 2014). Increased glutamate neurotransmission can result in damage to the SN DA system by causing axonal degeneration. As seen in Fig. 5*B*, a 2 (genotype) × 2 (age) ANOVA found that there was a significant effect of age on GLT-1 levels in the striatum ($F_{(1,18)}$=6.442; p<0.05). There was also a trend towards a genotype by age interaction; however, this was not significant ($F_{(1,18)}$=4.225; p=0.0546). A group-wise comparison demonstrated a significant difference between groups ($F_{(3,18)}$=3.895; p<0.05). A Fisher's PLSD post-hoc analysis showed that at 12 mon, *Gdnf*$^{+/-}$ mice had significantly lower GLT-1 levels than both 8 mon *Gdnf*$^{+/-}$ mice (p<0.01) and 12 mon WT mice (p<0.05; Fig. 5*B*). Since there is no significant difference between genotypes at 8 mon, the decrease of GLT-1 in the striatum occurs after the alterations of glutamate in the SN.

GFAP protein levels were measured to assess astrogliosis in the striatum (Fig. 5*C*). A 2 (genotype) × 2 (age) ANOVA revealed genotype and age effects on GFAP levels in the striatum ($F_{(1,20)}$=10.539; p<0.01 and $F_{(1,20)}$=18.398; p<0.001, respectively), but there was not a significant interaction. A group-wise comparison showed that the groups are significantly different ($F_{(3,20)}$=9.357; p<0.001). A Fisher's PLSD post-hoc analysis indicated that GFAP was lower in 8 mon mice than in 12 mon mice, regardless of genotype (*Gdnf*$^{+/-}$: p<0.01; WT: p<0.01). *Gdnf*$^{+/-}$ mice had higher GFAP levels at both ages than their WT counterparts (8 mon: p<0.05; 12 mon: p<0.05; Fig. 5*C*). These data show astrogliosis in the striatum of both genotypes with age, but to a greater extent in *Gdnf*$^{+/-}$ mice. Decreased GLT-1 levels and increased GFAP levels potentially suggest the presence of glutamate system alterations in the dorsal striatum that occur prior to the DAergic degeneration seen in *Gdnf*$^{+/-}$ mice, providing a potential mechanism of degeneration.

4. Discussion

Results from these studies demonstrate that changes in glutamate signaling are seen earlier than the DAergic neuron loss and motor impairments observed in *Gdnf*$^{+/-}$ mice (Boger et al., 2006; Littrell et al., 2013). Our findings include higher basal glutamate levels and increased glutamate release, lower levels of GLT-1-ir and higher levels of GFAP-ir in the SN of *Gdnf*$^{+/-}$ mice. Despite the increase of GFAP in the striatum at 12 mon in both genotypes, the glial transporter GLT-1 is expressed at significantly lower levels in the striatum of 12 mon *Gdnf*$^{+/-}$ mice. *This finding suggests that the change in GLT-1 is due to a reduction in the expression of GLT-1, as opposed to an alteration in GLT-1 function. Astrogliosis, known to increase with normal aging (*Lim et al., 2000*), has been shown to alter genetic expression in astrocytes (*Sofroniew 2009*). Elevated GFAP-ir in 8 mon Gdnf*$^{+/-}$ *mice shows that astrogliosis is occurring earlier in these mice compared to WT counterparts. This coupled with the reduction of GLT-1-ir in 8 mon* Gdnf$^{+/-}$ *mice indicates that astrogliosis leads to a reduction in expression of the of the glial glutamate transporter GLT-1. This pattern of astrogliosis paired with decreased GLT-1-ir is seen again in 12 mon mice of both genotypes. Future studies, including RT-PCR for mRNA and uptake assays, are warranted to determine the exact nature of this change in expression.*

We have previously demonstrated that by 12 mon of age, *Gdnf*$^{+/-}$ mice have reduced motor activity and an accelerated loss of SN DA neurons (Boger et al., 2006); however, the mechanism by which this occurs is unknown. One potential mechanism is glutamate excitotoxicity. Glutamate neurons in the STN project to the SN, and it has been hypothesized that dysregulation of glutamate neurotransmission results in excess glutamate stimulating post-synaptic receptors and increased Ca^{2+} influx, *potentially* leading to cell death. This study sought to establish a potential link between disrupted glutamate signaling and GDNF levels. This was accomplished by examining glutamate transmission in *Gdnf*$^{+/-}$ mice. Although the full mechanism by which excitotoxicity may occur is unknown, two potential causes are: 1) increased glutamate release from the presynaptic cells; or 2) alterations in the function or expression of the transporter that removes glutamate from the synapse.

In this study, we demonstrated that at 8 mon of age, *Gdnf*$^{+/-}$ mice have higher basal levels of glutamate compared to age-matched WT mice. This is an age prior to the onset of motoric and DAergic loss *previously* observed in these mice (Boger et al., 2006). Previous studies have demonstrated that excess glutamate in the synaptic cleft can set the stage for increased post-synaptic receptor activation. In addition to having increased basal levels of glutamate at 8 mon, *Gdnf*$^{+/-}$ mice also displayed increased KCl-stimulated release of glutamate. Based on previous studies, both higher basal levels of glutamate and increased stimulated release coupled together *could* result in a potential excitotoxic environment for the SN DA neurons in *Gdnf*$^{+/-}$ mice. Future studies will be conducted to determine the exact age that glutamate neurotransmission becomes altered and delve into the downstream effects as a result of increased extracellular glutamate. However, by 12 mon — the age at which we have previously shown that SN DA neurons are decreased in *Gdnf*$^{+/-}$ mice (Boger et al., 2006) — KCl-stimulated glutamate release is reduced compared to WT mice. One possible reason

for this reduction is the loss of glutamate neurons in the STN, which we demonstrated in 12 mon *Gdnf*$^{+/-}$ mice during this study.

Another potential mechanism for excess extracellular glutamate is a lack of clearance via glutamate transporters (Fischer et al., 2013; Russo et al., 2013). While no significant differences were observed at 8 mon of age, at 12 mon, *Gdnf*$^{+/-}$ mice had significantly slower uptake of glutamate in the SN. This finding was coupled with reduced immunoreactivity of GLT-1, the major transporter associated with glutamate uptake into astrocytes, in the SN. Similarly, at 12 mon, in the dorsal striatum of *Gdnf*$^{+/-}$ mice, we showed that GLT-1 levels were lower and GFAP levels were higher compared to age-matched WT mice.

To determine the potential role of glutamate-induced damage in the dorsal striatum (the target region for SN DA neurons), we assessed TH levels. These studies showed lower levels of TH in 12 mon *Gdnf*$^{+/-}$ mice compared to age-matched WT and 8 mon mice, regardless of genotype. These findings are consistent with our previous studies showing reduced TH-positive cells in the SN of 12 mon *Gdnf*$^{+/-}$ mice (Boger et al., 2006; Littrell et al., 2013).

These data show two separate mechanisms of glutamate excitotoxicity, increased release and decreased uptake. While we are still working on the mechanism of increased release, the decreased uptake can be explained by lower levels of GLT-1 in the SN and dorsal striatum. These changes in glutamate neurotransmission are initially seen at 8 mon in *Gdnf*$^{+/-}$ mice, whereas the reduction of striatal TH is not observed until 12 mon. *In this study, we see that mice with a GDNF deficiency have altered glutamate signaling that precedes an accelerated decline of the nigrostriatal pathway.* This accelerated decline then leads to motor dysfunction, according to our previous studies (Boger et al., 2006; Littrell et al., 2013).

5. Conclusions

Taken together, these data show that excess release from STN glutamatergic neurons, as well as reduced glutamate uptake by GLT-1, may contribute to excitotoxicity that eventually leads to DAergic cell death. Future studies will be conducted to determine *whether changes in glutamate kinetics are the cause of DAergic neuronal death*, the mechanism by which glutamate release is greater in *Gdnf*$^{+/-}$ mice, and to determine whether GDNF-like compounds alleviate these deficiencies.

Acknowledgments

This work was supported by a grant from the MUSC Barmore Fund and NIH/NIA grant 4R00AG033687.

References

Blandini F, Porter RH, Greenamyre JT. Glutamate and Parkinson’s disease. Mol Neurobiol. 1996; 12(1):73–94.10.1007/BF02740748 [PubMed: 8732541]

Boger HA, Middaugh LD, Huang P, Zaman V, Smith AC, Hoffer BJ, Tomac AC, Granholm AC. A partial GDNF depletion leads to earlier age-related deterioration of motor function and tyrosine

hydroxylase expression in the substantia nigra. Exp Neurol. 2006; 202(2):336–47.10.1016/j.expneurol.2006.06.006 [PubMed: 16889771]

Boger HA, Middaugh LD, Patrick KS, Ramamoorthy S, Denehy ED, Zhu H, Pacchioni AM, Granholm AC, McGinty JF. Long-term consequences of methamphetamine exposure in young adults are exacerbated in glial cell line-derived neurotrophic factor heterozygous mice. J Neurosci. 2007; 27(33):8816–25.10.1523/JNEUROSCI.1067-07.2007 [PubMed: 17699663]

Borlongan CV, Zhou FC, Hayashi T, Su TP, Hoffer BJ, Wang Y. Involvement of GDNF in neuronal protection against 6-OHDA-induced parkinsonism following intracerebral transplantation of fetal kidney tissues in adult rats. Neurobiol Dis. 2001; 8(4):636–46.10.1006/nbdi.2001.0410 [PubMed: 11493028]

Burmeister JJ, Gerhardt GA. Self-referencing ceramic-based multisite microelectrodes for the detection and elimination of interferences from the measurement of L-glutamate and other analytes. Anal Chem. 2001; 73(5):1037–42. [PubMed: 11289414]

Burmeister JJ, Pomerleau F, Palmer M, Day BK, Huettl P, Gerhardt GA. Improved ceramic-based multisite microelectrode for rapid measurements of L-glutamate in the CNS. J Neurosci Methods. 2002; 119(2):163–71. [PubMed: 12323420]

Chauhan NB, Siegel GJ, Lee JM. Depletion of glial cell line-derived neurotrophic factor in substantia nigra neurons of Parkinson's disease brain. J Chem Neuroanat. 2001; 21(4):277–88. [PubMed: 11429269]

Deister C, Schmidt CE. Optimizing neurotrophic factor combinations for neurite outgrowth. J Neural Eng. 2006; 3(2):172–9.10.1088/1741-2560/3/2/011 [PubMed: 16705273]

Di Liberto V, Mudò G, Belluardo N. mGluR2/3 agonist LY379268, by enhancing the production of GDNF, induces a time-related phosphorylation of RET receptor and intracellular signaling Erk1/2 in mouse striatum. Neuropharmacology. 2011; 61(4):638–45.10.1016/j.neuropharm.2011.05.006 [PubMed: 21619889]

Favier M, Carcenac C, Drui G, Boulet S, El Mestikawy S, Savasta M. High-frequency stimulation of the subthalamic nucleus modifies the expression of vesicular glutamate transporters in basal ganglia in a rat model of Parkinson's disease. BMC Neurosci. 2013; 14:152.10.1186/1471-2202-14-152 [PubMed: 24308494]

Fieblinger T, Sebastianutto I, Alcacer C, Bimpisidis Z, Maslava N, Sandberg S, Engblom D, Cenci MA. Mechanisms of Dopamine D1 Receptor-Mediated ERK1/2 Activation in the Parkinsonian Striatum and Their Modulation by Metabotropic Glutamate Receptor Type 5. J Neurosci. 2014; 34(13):4728–40.10.1523/JNEUROSCI.2702-13.2014 [PubMed: 24672017]

Fischer KD, Houston AC, Rebec GV. Role of the major glutamate transporter GLT1 in nucleus accumbens core versus shell in cue-induced cocaine-seeking behavior. J Neurosci. 2013; 33(22):9319–27.10.1523/JNEUROSCI.3278-12.2013 [PubMed: 23719800]

Franklin, KBJ.; Paxinos, G. The Mouse Brain in Stereotaxic Coordinates. 2. Academic Press; San Diego, CA: 2001.

Gianforcaro A, Hamadeh MJ. Vitamin D as a potential therapy in amyotrophic lateral sclerosis. CNS Neurosci Ther. 2014; 20(2):101–11.10.1111/cns.12204 [PubMed: 24428861]

Gill SS, Patel NK, Hotton GR, O'Sullivan K, McCarter R, Bunnage M, Brooks DJ, Svendsen CN, Heywood P. Direct brain infusion of glial cell line-derived neurotrophic factor in Parkinson disease. Nat Med. 2003; 9(5):589–95.10.1038/nm850 [PubMed: 12669033]

Gordon PH. Amyotrophic Lateral Sclerosis: An update for 2013 Clinical Features, Pathophysiology, Management and Therapeutic Trials. Aging Dis. 2013; 4(5):295–310.10.14336/AD.2013.0400295 [PubMed: 24124634]

Hascup KN, Hascup ER, Pomerleau F, Huettl P, Gerhardt GA. Second-by-second measures of L-glutamate in the prefrontal cortex and striatum of freely moving mice. J Pharmacol Exp Ther. 2008; 324(2):725–31.10.1124/jpet.107.131698 [PubMed: 18024788]

Ho A, Gore AC, Weickert CS, Blum M. Glutamate regulation of GDNF gene expression in the striatum and primary striatal astrocytes. Neuroreport. 1995; 6(10):1454–8. [PubMed: 7488747]

Hoffman AF, Gerhardt GA. In vivo electrochemical studies of dopamine clearance in the rat substantia nigra: effects of locally applied uptake inhibitors and unilateral 6-hydroxydopamine lesions. J Neurochem. 1998; 70(1):179–89. [PubMed: 9422361]

Ingram DK. Age-related decline in physical activity: generalization to nonhumans. Med Sci Sports Exerc. 2000; 32(9):1623–9. [PubMed: 10994915]

Iribe Y, Moore K, Pang KC, Tepper JM. Subthalamic stimulation-induced synaptic responses in substantia nigra pars compacta dopaminergic neurons in vitro. J Neurophysiol. 1999; 82(2):925–33. [PubMed: 10444687]

Jankovic J. Parkinson's disease: clinical features and diagnosis. J Neurol Neurosurg Psychiatry. 2008; 79(4):368–76.10.1136/jnnp.2007.131045 [PubMed: 18344392]

Jenner P, Olanow CW. Understanding cell death in Parkinson's disease. Ann Neurol. 1998; 44(3 Suppl 1):S72–84. [PubMed: 9749577]

Joseph JA, Fisher DR, Strain J. Muscarinic receptor subtype determines vulnerability to oxidative stress in COS-7 cells. Free Radic Biol Med. 2002; 32(2):153–61. [PubMed: 11796204]

Kosuge Y, Sekikawa-Nishida K, Negi H, Ishige K, Ito Y. Characterization of chronic glutamate-mediated motor neuron toxicity in organotypic spinal cord culture prepared from ALS model mice. Neurosci Lett. 2009; 454(2):165–9.10.1016/j.neulet.2009.03.017 [PubMed: 19429077]

Kruman II, Mattson MP. Pivotal role of mitochondrial calcium uptake in neural cell apoptosis and necrosis. J Neurochem. 1999; 72(2):529–40. [PubMed: 9930724]

Lim GP, Yang F, Chu T, Chen P, Beech W, Teter B, Tran T, Ubeda O, Ashe KH, Frautschy SA, Cole GM. Ibuprofen suppresses plaque pathology and inflammation in a mouse model for Alzheimer's disease. J Neurosci. 2000; 20(15):5709–14. [PubMed: 10908610]

Lin LF, Doherty DH, Lile JD, Bektesh S, Collins F. GDNF: a glial cell line-derived neurotrophic factor for midbrain dopaminergic neurons. Science. 1993; 260(5111):1130–2. [PubMed: 8493557]

Littrell OM, Granholm AC, Gerhardt GA, Boger HA. Glial cell-line derived neurotrophic factor (GDNF) replacement attenuates motor impairments and nigrostriatal dopamine deficits in 12-month-old mice with a partial deletion of GDNF. Pharmacol Biochem Behav. 2013; 104:10–9.10.1016/j.pbb.2012.12.022 [PubMed: 23290934]

Manev H, Favaron M, Guidotti A, Costa E. Delayed increase of Ca2+ influx elicited by glutamate: role in neuronal death. Mol Pharmacol. 1989; 36(1):106–12. [PubMed: 2568579]

Mark KA, Soghomonian JJ, Yamamoto BK. High-dose methamphetamine acutely activates the striatonigral pathway to increase striatal glutamate and mediate long-term dopamine toxicity. J Neurosci. 2004; 24(50):11449–56.10.1523/JNEUROSCI.3597-04.2004 [PubMed: 15601951]

McGrath J, Lintz E, Hoffer BJ, Gerhardt GA, Quintero EM, Granholm AC. Adeno-associated viral delivery of GDNF promotes recovery of dopaminergic phenotype following a unilateral 6-hydroxydopamine lesion. Cell Transplant. 2002; 11(3):215–27. [PubMed: 12075987]

Misonou Y, Asahi M, Yokoe S, Miyoshi E, Taniguchi N. Acrolein produces nitric oxide through the elevation of intracellular calcium levels to induce apoptosis in human umbilical vein endothelial cells: implications for smoke angiopathy. Nitric Oxide. 2006; 14(2):180–7.10.1016/j.niox.2005.09.004 [PubMed: 16275026]

Pichel JG, Shen L, Sheng HZ, Granholm AC, Drago J, Grinberg A, Lee EJ, Huang SP, Saarma M, Hoffer BJ, Sariola H, Westphal H. Defects in enteric innervation and kidney development in mice lacking GDNF. Nature. 1996; 382(6586):73–6.10.1038/382073a0 [PubMed: 8657307]

Quintero JE, Pomerleau F, Huettl P, Johnson KW, Offord J, Gerhardt GA. Methodology for rapid measures of glutamate release in rat brain slices using ceramic-based microelectrode arrays: basic characterization and drug pharmacology. Brain Res. 2011; 1401:1–9.10.1016/j.brainres.2011.05.025 [PubMed: 21664606]

Russo R, Cavaliere F, Varano GP, Milanese M, Adornetto A, Nucci C, Bonanno G, Morrone LA, Corasaniti MT, Bagetta G. Impairment of neuronal glutamate uptake and modulation of the glutamate transporter GLT-1 induced by retinal ischemia. PLoS One. 2013; 8(8):e69250.10.1371/journal.pone.0069250 [PubMed: 23936321]

Slevin JT, Gerhardt GA, Smith CD, Gash DM, Kryscio R, Young B. Improvement of bilateral motor functions in patients with Parkinson disease through the unilateral intraputaminal infusion of glial cell line-derived neurotrophic factor. J Neurosurg. 2005; 102(2):216–22.10.3171/jns.2005.102.2.0216 [PubMed: 15739547]

Smith, PJS.; Sanger, RH.; Messerli, MA. Principles, Development and Applications of Self-Referencing Electrochemical Microelectrodes to the Determination of Fluxes at Cell Membranes.

In: Michael, AC.; Borland, LM., editors. Electrochemical Methods for Neuroscience. CRC Press; Boca Raton, FL: 2007.

Sofroniew MV. Molecular dissection of reactive astrogliosis and glial scar formation. Trends Neurosci. 2009; 32(12):638–47.10.1016/j.tins.2009.08.002 [PubMed: 19782411]

Sonsalla PK, Giovanni A, Sieber BA, Donne KD, Manzino L. Characteristics of dopaminergic neurotoxicity produced by MPTP and methamphetamine. Ann N Y Acad Sci. 1992; 648:229–38. [PubMed: 1637048]

Varoqui H, Schäfer MK, Zhu H, Weihe E, Erickson JD. Identification of the differentiation-associated Na+/PI transporter as a novel vesicular glutamate transporter expressed in a distinct set of glutamatergic synapses. J Neurosci. 2002; 22(1):142–55. [PubMed: 11756497]

Volkow ND, Gur RC, Wang GJ, Fowler JS, Moberg PJ, Ding YS, Hitzemann R, Smith G, Logan J. Association between decline in brain dopamine activity with age and cognitive and motor impairment in healthy individuals. Am J Psychiatry. 1998; 155(3):344–9. [PubMed: 9501743]

Highlights

- A partial reduction of GDNF caused increased glutamate release at a time point when other studies have suggested that there is not yet significant dopamine loss or motor impairment.
- *Gdnf*$^{+/-}$ mice displayed increased astrogliosis in the substantia nigra and striatum with age, compared to wildtype mice.
- Reduced GDNF resulted in decrease glutamate uptake in the substantia nigra as well as reduced levels of the astrocytic glutamate transporter, GLT-1.

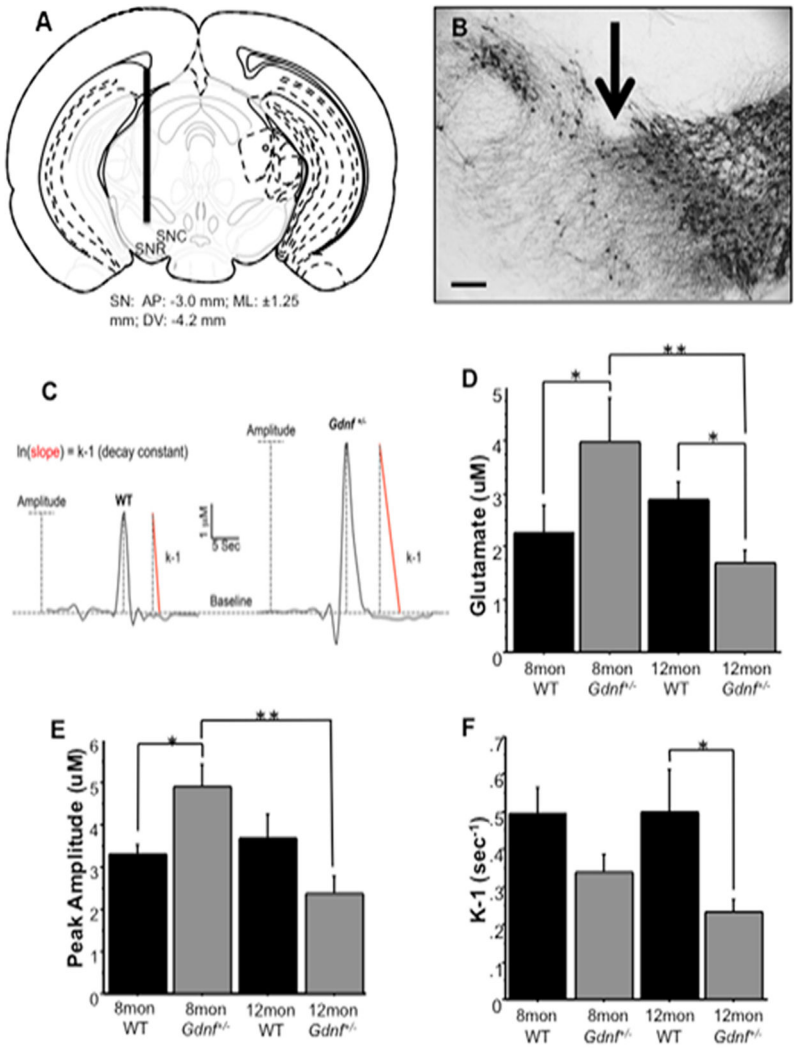

Figure 1.

Glutamate kinetics were measured in the substantia nigra of 8 mon and 12 mon WT and *Gdnf*$^{+/-}$ mice. ***A***, *Microelectrode placement through the mouse substantia nigra. The diagrams show the approximate location of the microelectrode at: AP-3.0 (relative to bregma; modified from* Franklin and Paxinos (2001)). ***B***, *Photomicrograph of TH-ir in the SN depicting electrode placement (arrow) in mice.* ***C***, *Representative traces of glutamate kinetics in 8 mon old WT and Gdnf*$^{+/-}$ *mice to depict the various measures assessed, including amplitude (dotted line) and k-1 (red slope line).* **D**, Basal levels of glutamate decreased in *Gdnf*$^{+/-}$ mice over time (**p<0.01). At 8 mon, *Gdnf*$^{+/-}$ mice had higher levels of glutamate than WT animals (*p<0.05), and at 12 mon, basal levels dropped in *Gdnf*$^{+/-}$ mice below those of WT animals (*p<0.05). ***E***, The amount of glutamate released in response to 70 mM KCl stimulation decreased in *Gdnf*$^{+/-}$ mice over time (**p<0.01). At 8 mon, *Gdnf*$^{+/-}$ mice released more glutamate than WT animals during KCl-stimulations (*p<0.05). ***F***, Glutamate uptake was slower in 12 mon *Gdnf*$^{+/-}$ mice than in WT age-matched animals (*p<0.05). Scale bar=150uM.

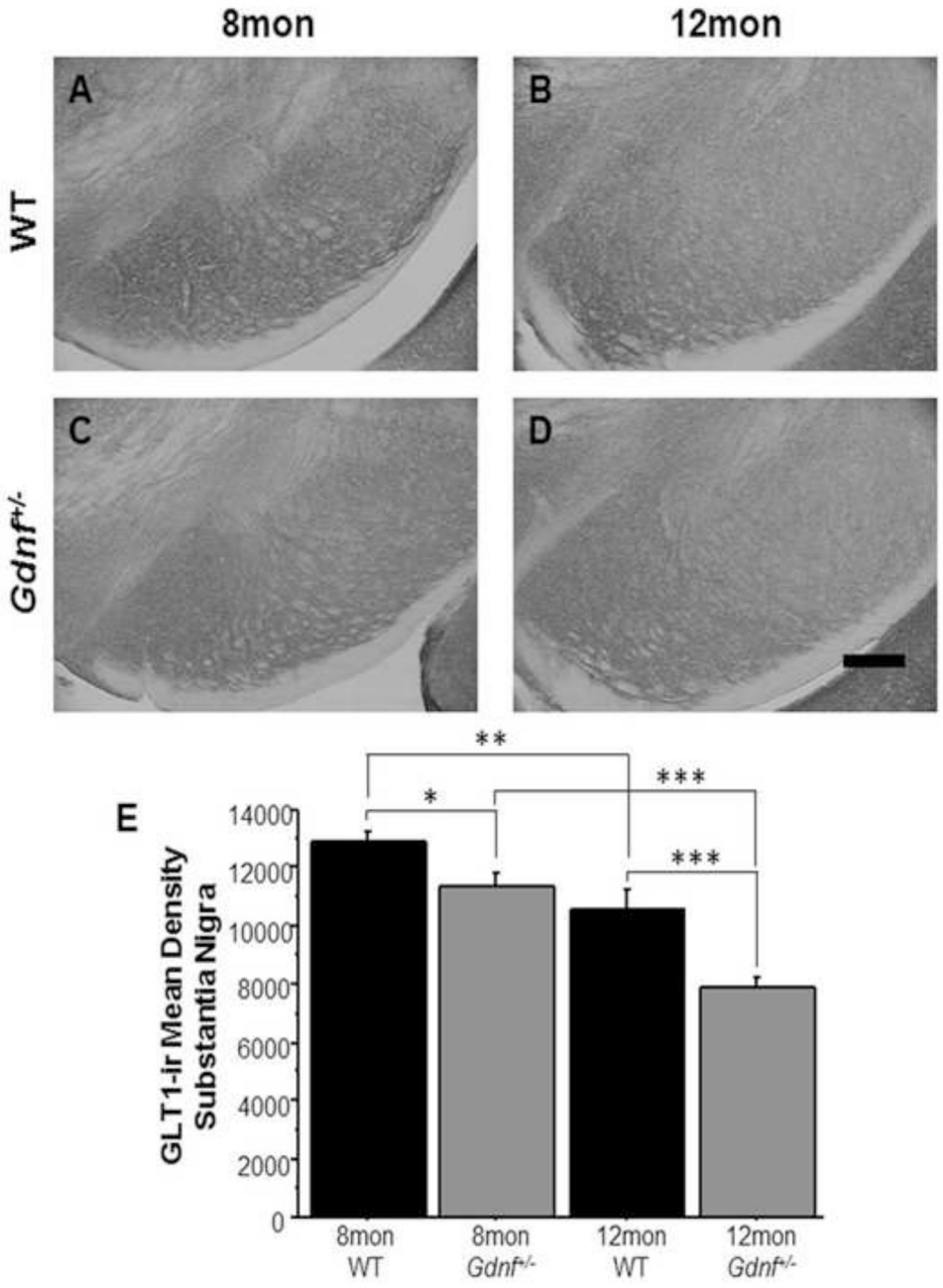

Figure 2.

GLT-1-ir was lower in *Gdnf*$^{+/-}$ mice at both ages. ***A–D***, Photomicrographs (10×) in SN of 8 mon WT mice (***A***), 12 mon WT mice (***B***), 8 mon *Gdnf*$^{+/-}$ mice (***C***), and 12 mon *Gdnf*$^{+/-}$ mice (***D***). ***E***, GLT-1-ir decreased in both genotypes with age (WT: **p<0.01, *Gdnf*$^{+/-}$: ***p<0.001), but overall was lower in *Gdnf*$^{+/-}$ mice at both ages (8 mon: *p<0.05, 12 mon: ***p<0.001). Scale bar=200uM.

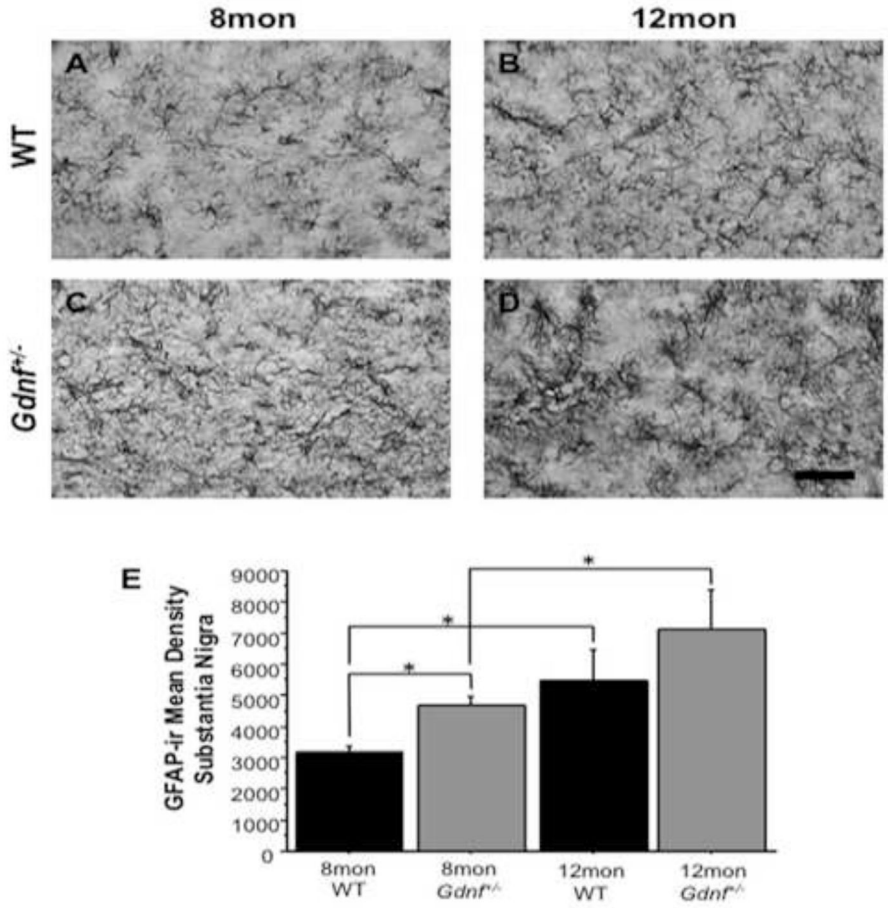

Figure 3.

GFAP-ir increased with age in both genotypes. ***A–D***, Photomicrographs (60×) in SN of 8 mon WT mice (***A***), 12 mon WT mice (***B***), 8 mon *Gdnf*$^{+/-}$ mice (***C***), and 12 mon *Gdnf*$^{+/-}$ mice (***D***). ***E***, GFAP-ir increased with age in both WT (*p<0.05) and *Gdnf*$^{+/-}$ mice (*p<0.05). However, GFAP-ir was significantly greater in the SN of *Gdnf*$^{+/-}$ mice compared to WT counterparts (*p<0.05). Scale bar=0.5mm.

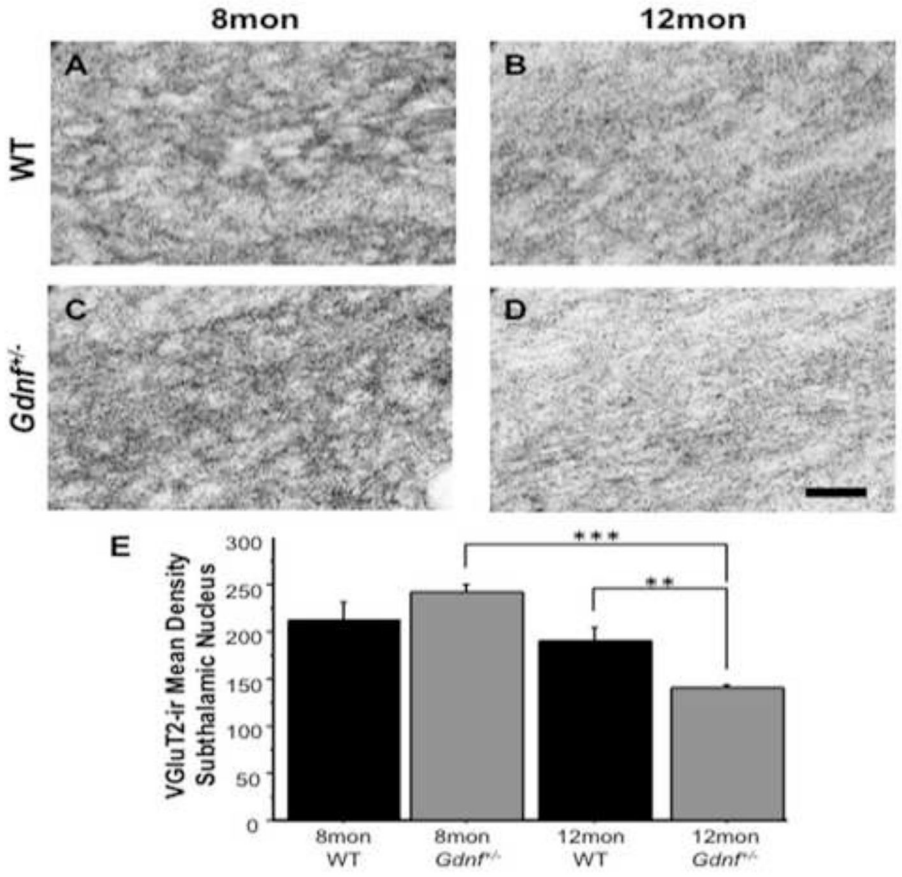

Figure 4.

VGLUT-2-ir, an indicator of glutamatergic neurons, decreased over time in the STN of *Gdnf*$^{+/-}$ mice. ***A–D***, Photomicrographs of VGLUT-2-ir (60×) in STN of 8 mon WT mice (***A***), 12 mon WT mice (***B***), 8 mon *Gdnf*$^{+/-}$ mice (***C***), and 12 mon *Gdnf*$^{+/-}$ mice (***D***). ***E***, VGLUT-2-ir decreased significantly between and 8 mon and 12 mon *Gdnf*$^{+/-}$ mice (***p<0.001) and at 12 mon was significantly lower than WT littermates (**p<0.01). Scale bar=0.5mm.

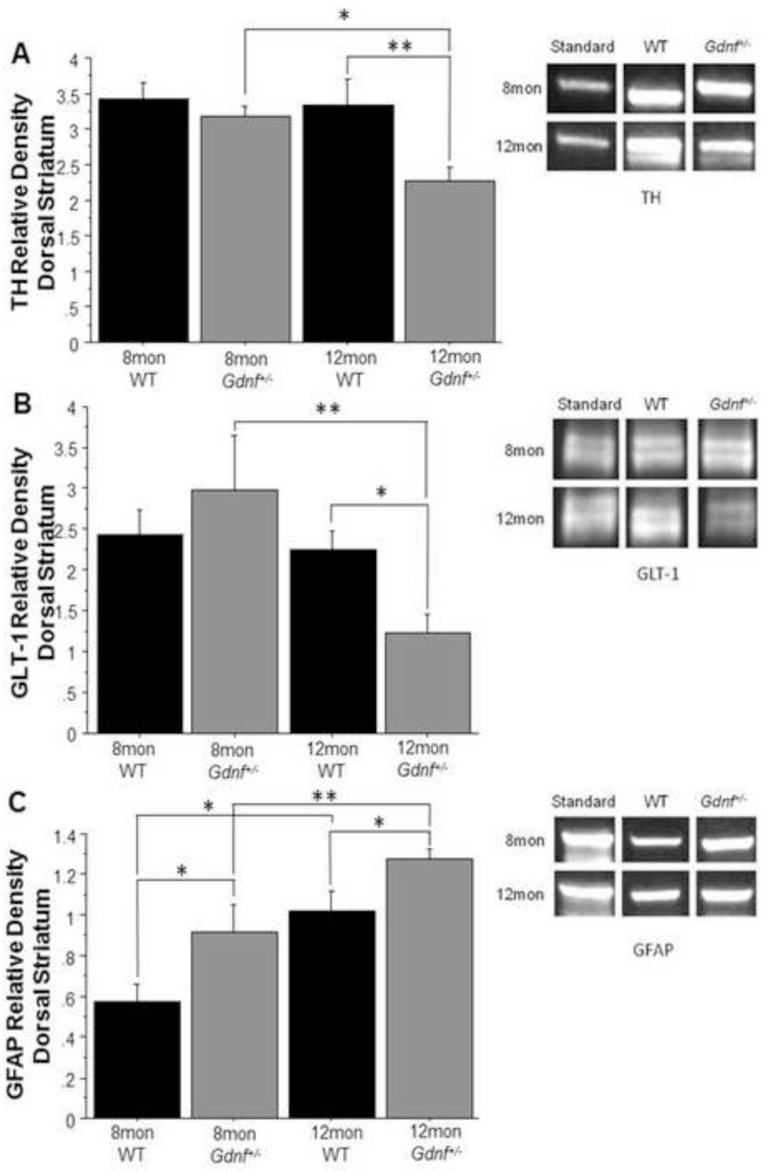

Figure 5.

Striatal Protein levels of TH, GLT-1 and GFAP were altered in *Gdnf*$^{+/-}$ mice. (***A)*** TH protein levels decreased in 12 mon *Gdnf*$^{+/-}$ mice from both 8 mon *Gdnf*$^{+/-}$ mice (*p<0.05) and 12 mon WT mice (**p<0.01). (***B***) GLT-1 protein levels were lower in 12 mon *Gdnf*$^{+/-}$ mice than either 8 mon *Gdnf*$^{+/-}$ mice (**p<0.01) or 12 mon WT mice (*p<0.05). (***C***) GFAP was increased predictably with age in both genotypes (WT: *p<0.05, *Gdnf*$^{+/-}$: **p<0.01). GFAP levels were higher in *Gdnf*$^{+/-}$ mice at both ages compared to WT littermates (8 mon: *p<0.05, 12 mon: *p<0.05).